JACS Au
AN OPEN ACCESS JOURNAL OF THE AMERICAN CHEMICAL SOCIETY

pubs.acs.org/jacsau
Article

Intermolecular Stacking-Instructed Chiral Preference in Covalent 2 + 2 Macrocyclization

Zhen-Sheng Huang,[#] Wen-Rong Wang,[#] Fang-Hong Yang, Fei Gou, Liuyin Jiang,* Chi-Cheng Qiu, Yang-Yu Tai, Xiao-Sheng Yan, Xin Wu,* Tao Jiang,* and Yun-Bao Jiang*

Cite This: JACS Au 2026, 6, 1319−1326

ABSTRACT: We report the discovery of unexpected chiral preferences in 2 + 2 macrocyclization, where a racemic pair of 2,6-pyridine(dicarbonylamino-acid)hydrazides or two equiv of the meso analogue are reacted with two molecules of achiral, structurally symmetric bidentate, 1,4-pheylenediisothiocyanate. Using racemic alanine (A)-based dihydrazides L,L-AA and D,D-AA as reactants, heterochiral macrocycle L,L,D,D-AAAA forms exclusively in ca. 80% yield in acetonitrile/DMF at 110 °C, with no detectable formation of homochiral L,L,L,L- or D,D,D,D-counterparts. This heterochiral preference extends to other amino acid residues, as demonstrated by the selective formation of L,L,D,D-FFFF and L,L,D,D-/D,D,L,L-AAFF when employing phenylalanine (F)-based or mixed F- and A-based dihydrazides. Surprisingly, when meso dihydrazide L,D-AA is used, a strong preference for forming L,D,D,L-AAAA over L,D,L,D-AAAA was observed. Despite being hetero- and homochiral of the two amino acid residues in the 1,4-benzenediamidothiourea edges, the two kinds of the preferred macrocycles, L,L,D,D-AAAA and L,D,D,L-AAAA, share the same configurations of four edges: parallel LL/DD and LD/LD. This chiral preference arises from the enhanced intermacrocycle stacking. Structural analyses reveal that both L,L,D,D-AAAA and L,D,D,L-AAAA exhibit more symmetric molecular conformations upon stacking compared to L,L,L,L-AAAA and L,D,L,D-AAAA. These distinct structural features lead to a 30−40 °C increase in decomposition temperature for the favored macrocycles. Being orthogonal to most reported entropy-driven homochiral preferences that rely on intramolecular bonding, this study establishes a new scheme to leverage intermolecular interactions for covalent, catalyst-free stereoselective macrocyclization.

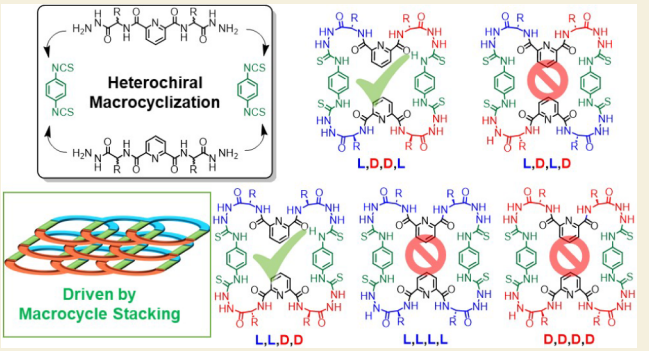

KEYWORDS: *chiral self-sorting, peptidomimetic macrocycles, stereoselective macrocyclization, macrocycle stacking, anion receptor*

INTRODUCTION

The natural homochirality such as the exclusive presence of L-amino acids in peptides and D-sugars in nucleic acids continues to fascinate the explorations of its origin[1] and inspire the rational control of enantioselectivity in synthetic chemistry. The homochirality implies that in prebiotic polymer formation, one chiral unit present in a reaction intermediate favors the incorporation of further units of the same chirality. As seen in peptides or DNA molecules, neighboring amino acid residues or sugar moieties are linked via linear covalent backbones, which might not be sufficient to bias homochiral polymer formation. There shall be additional interactions between the neighboring chiral centers, which means that multivalent interactions are needed at some stage in the formation of the linkage between the neighboring chiral units. Cyclic structure is an immediate candidate in that context. Indeed, homochirality has been observed during cyclization, leading to chiral cyclic compounds such as macrocycles,[2] cages[3,4] and knots[5] consisting of either rigid or flexible building blocks. It is noted that in the majority of the reported homochiral cyclic structures, the building blocks are linked via dynamic covalent bonds such as the imine bond (−CH═N−), while few cases are reported with permanent bonds under catalytic reaction conditions.[2e] Note that an information theory has been applied to well explain the observed homochirality,[2e,4c,d] in that the homochiral product molecule is of a higher entropy, while its enthalpy is similar to that of the heterochiral product. A very nice experiment to support this explanation is the observation of the heterochiral macrocycle from a metathesis reaction at lower temperatures, at which the contribution of entropy is reduced.[2e] We noted that in all those cases of forming homochiral macrocyclic products, they exist in solution as molecularly dissolved species. In those cases,

Received: December 10, 2025
Revised: January 22, 2026
Accepted: February 2, 2026
Published: February 9, 2026

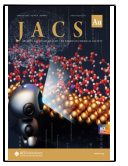

intramolecular interaction has been the focus for understanding the chirality communication in the transition states, the majority of which are cyclic structures or contain cyclic structures,[6] and/or the chirality of the final product.

It is therefore natural to wonder what would happen with the reactions of chiral species if the intermolecular interactions between the chiral products are strong. We thus launched to explore the cyclization reactions that the chiral cyclic product molecules would interact so strongly that they exist in the aggregate forms, even appearing as visible precipitates or crystals (Scheme 1). We chose our recently developed

Scheme 1. Biasing the Outcome of a Macrocyclization Reaction (Using LL and DD Racemates as Building Units) via Strong Intermolecular Stacking of a Particular Stereoisomer (LLDD) among Possible Macrocyclic Products (LLDD, LLLL and DDDD)[a]

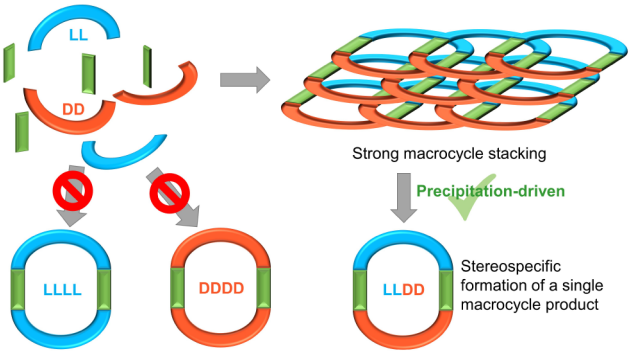

[a]Similarly, we observed the preferential formation of an LDDL over an LDLD macrocycle when an LD building unit was used.

macrocyclization reaction involving enantiopure reactants,[7] which resulted in precipitated products with strong intermolecular hydrogen bonding interactions. Reported herein is our discovery of the exclusive formation of the heterochiral macrocycles, the extralarge macrocycles, L,L,D,D-AAAA/FFFF/AAFF/FFAA (**1**-**4**) (Figure 1a), from the reaction of a racemic pair of dihydrazides of amino acid (A, F, or A+F) and achiral bidentate 1,4-phenylenediisothiocyanate in competitive solvent ACN/DMF at high reaction temperatures. Also of significance is that when a meso dihydride reactant L,D-AA was used, the only product formed at the high temperature of 110 °C was L,D,D,L-**1** but not L,D,L,D-**1** (Figure 1c), supporting the critical role of the product intermolecular interactions in directing the reaction pathway of the macrocyclization.

RESULTS AND DISCUSSION

We recently reported a facile access to the homochiral peptidomimetic large macrocycles (L,L,L,L- or D,D,D,D-**1**) from 2 molecules of enantiopure L,L- or D,D-Py$(AN_2H_3)_2$ in 1:1 (v/v) CH_3CN/DMF at 90 °C, in precipitates (cf. Figure 1a).[7] Crystal structure shows that the macrocyclic backbone is stabilized by a network of 8 hydrogen bonds that stabilize 4 β-turn structures, together with strong intermolecular hydrogen bonding that is responsible for the precipitation. It was therefore expected from such a multiple intramolecular hydrogen bonding network that a chirality communication within the cyclic structure may bias the product formation from the statistical distribution, when racemic dihydrides L,L- and D,D-Py$(AN_2H_3)_2$ are taken as the reactants, as also expected in the acyclic system.[8] As evidence for such chirality communication within the cyclic backbone in **1**, CD spectra of previously identified reaction intermediates, L,L- and D,D-Py$(ATUNCS)_2$ (structures shown in Figure 1b) were recorded in 98:2 (v/v) CH_3CN/DMSO (Figure S1). CD signals at 282 nm from the 4-(thioureido)phenylisothiocyanate chromophore (blue curves in Figure S1) were observed, which means that the terminal -NCS groups in the intermediate species are "chiral." This would lead to a chirality demand for the upcoming chiral reactant, which, in view of the chirality-assisted synthesis,[9] is likely in the homochiral manner.[9b]

Reactions of 1,4-Ph$(NCS)_2$ with 1.1 equiv of racemic mixtures of L,L- and D,D-Py$(AN_2H_3)_2$, under optimal conditions, 1:1 (v/v) DMF/CH_3CN at 90 °C, previously used for the synthesis of L,L,L,L- or D,D,D,D-**1**,[7] were therefore run at varying temperatures ranging from 25 to 120 °C. The products were found to precipitate from the reaction solution, too. ^{1}H NMR characterization (Figure 2) shows that, despite a statistical distribution of random reactions would result in a percentage and a maximum yield of 50% for L,L,D,D-**1**, the heterochiral product becomes increasingly dominant when reaction temperature increased beyond 90 °C, with yields substantially higher than 50% (Table 1). It is the only product at 110 °C in a yield of 81% by combining those from the precipitates and the solution phase, with no detectable homochiral L,L,L,L-**1** and D,D,D,D-**1**. This is different from the homochiral macrocyclic product expected in the chirality-assisted synthesis[9b] but instead forms an alternative enantiomer array.

Analysis of the heterochiral macrocyclic products both in the precipitates and in the solution from reaction at 90 °C reveals a slightly higher yield of heterochiral (39% for L,L,D,D-**1**) than that of the homochiral (L,L,L,L- and D,D,D,D-**1** at 37% in total) products, deviating slightly from the statistical product distribution (Table 1). At lower temperatures of 80 and 50 °C, practically statistical distribution was observed. This implies that at higher temperatures, a biased distribution would occur. Indeed, at an elevated reaction temperature above 90 °C, the heterochiral L,L,D,D-**1** started to dominate over the homochiral products, and a very high heterochiral-to-homochiral selectivity of 65:1 was found at 110 °C. Both heterochiral and homochiral macrocyclic products were found to dissociate at 120 °C, and therefore, higher temperature conditions were not tested. Further reaction optimization by heating the reaction mixtures in a pressure tube at 110 °C (solvothermal synthesis) for 16 h led to the exclusive formation of L,L,D,D-**1** in 81% yield, with no detectable homochiral products. For the solvothermal synthesis, it is worth pointing out that the reaction initially produced a small quantity (10%) of the homochiral macrocycles up to 12 h (Table 1 entry 8), which, however, completely disappeared when the reaction proceeded to 16 h. We also examined the possible dissociation and recombination[2e] of L,L,L,L-**1** and D,D,D,D-**1** under the optimal reaction conditions and found that no L,L,D,D-**1** was formed. This means that heterochiral L,L,D,D-**1** could not form via component exchange from L,L,L,L-**1** and D,D,D,D-**1**, demonstrating that the thiourea formation reaction is practically irreversible under our experimental conditions. These, together with the aforementioned observation that the heterochiral product was favored at higher temperatures (>100 °C), suggest that the product of the heterochiral macrocycle has a higher thermostability than the homochiral ones. This indicates stronger interactions between

https://doi.org/10.1021/jacsau.5c01669
JACS Au 2026, 6, 1319−1326

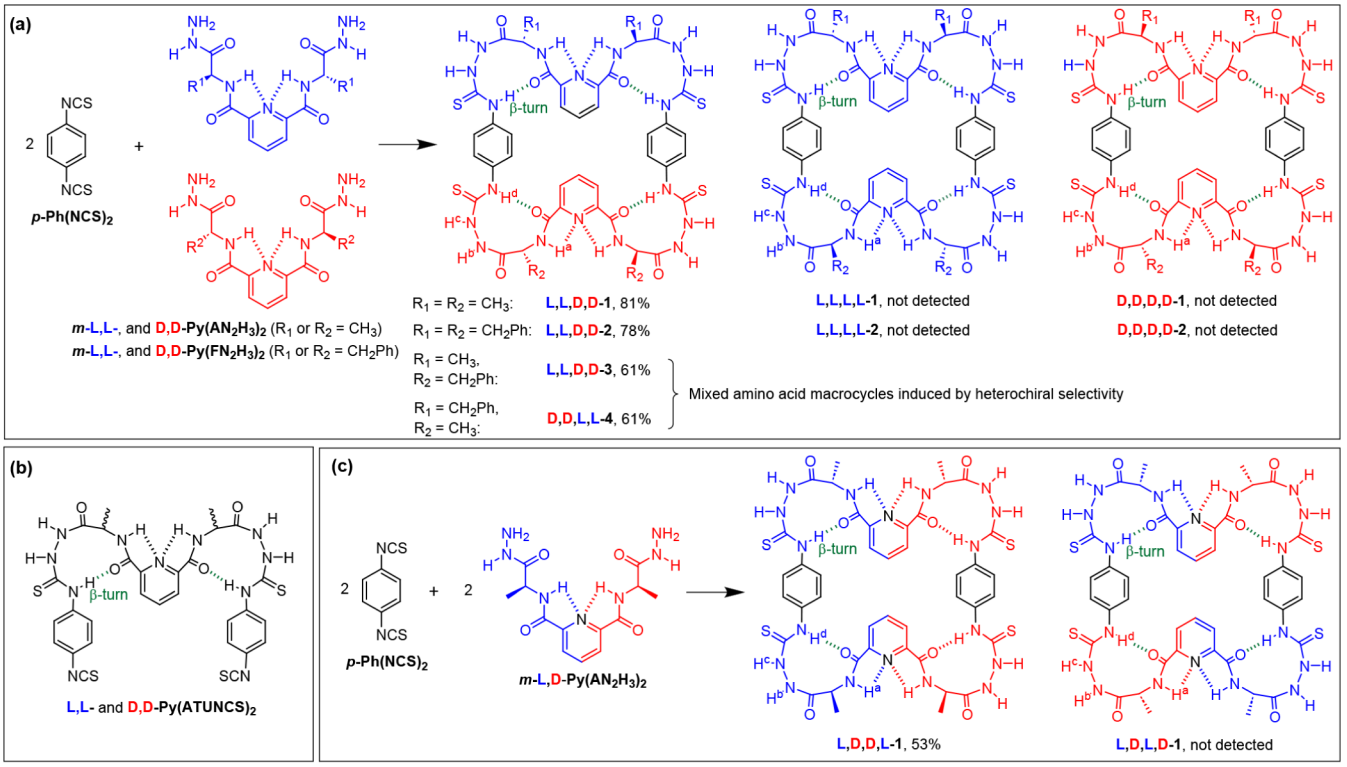

Figure 1. [2+2] Macrocyclization of 1,4-phenyldiisothiocyanate with racemic or meso 2,6-pyridinedicarbonylamino acid-based dihydrazides, giving diverse heterochiral macrocyclic products. (a) Selective formation of heterochiral same-amino-acid macrocycles L,L,D,D-**1** and L,L,D,D-**2** using alanine- or phenylalanine-based dihydrazides, and heterochiral mixed-amino-acid macrocycles L,L,D,D-**3** and D,D,L,L-**4** using combinations of dihydrazides bearing alanine or phenylalanine residues. (b) Structures of the reaction intermediates, L,L- and D,D-$(PyATUNCS)_2$. (c) Selective formation of L,D,D,L-**1** over L,D,L,D-**1** using a meso dihydrazide reactant, *m*-L,D-$Py(AN_2H_3)_2$. Dashed lines represent intramolecular hydrogen bonds.

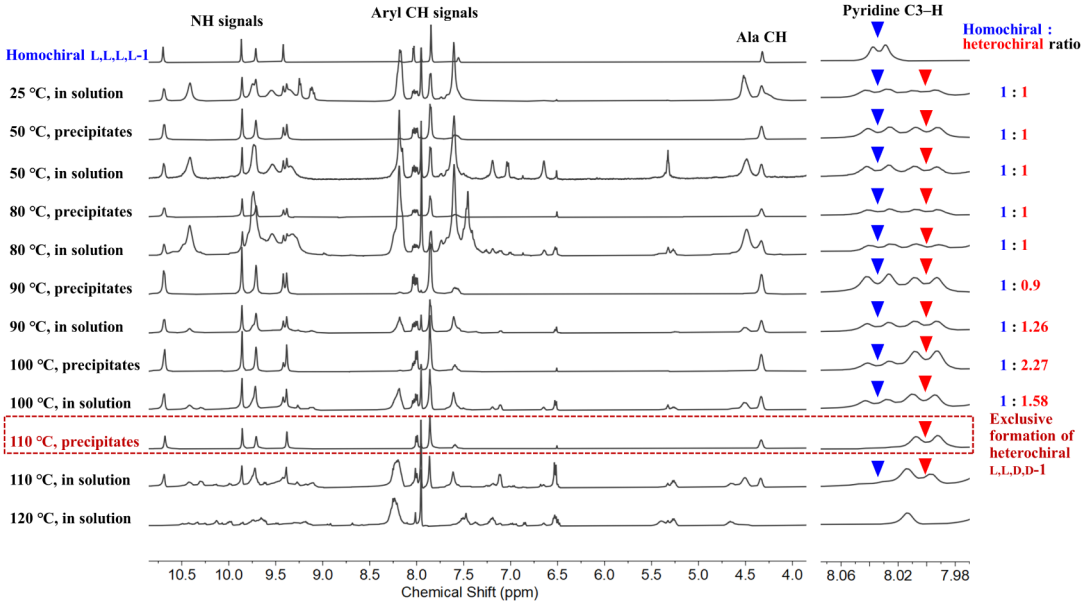

Figure 2. ^1H NMR traces of the precipitates (redissolved in DMSO-d_6) from the reaction of 1,4-$Ph(NCS)_2$ with a racemic mixture L,L- and D,D-$Py(AN_2H_3)_2$ (1.1 eq. each) in 1:1 (v/v) DMF/CH_3CN for 24 h conducted at different temperatures. The pyridine C3−H signals, observed at 8.03 ppm (blue triangle) from L,L,L,L-/D,D,D,D-**1** and at 8.00 ppm (red triangle) from L,L,D,D-**1**, are used to determine the molar ratio of homochiral (sum of L,L,L,L- and D,D,D,D-**1**) to heterochiral (L,L,D,D-**1**) products, shown on the right. See Table 1 for the product distribution in solution and in the precipitates.

the heterochiral macrocycles, accounting also for the observed predominant precipitation of the heterochiral products from the reaction solution, even at a high temperature of 110 °C, and the higher heterochiral preference in the precipitated products than in the products from the solution phase (Table 1). The precipitates were observed to be microcrystalline by

https://doi.org/10.1021/jacsau.5c01669
JACS Au 2026, 6, 1319−1326

Table 1. Yields of Hetero- (L,L,D,D-1) and Homochiral (L,L,L,L- and D,D,D,D-1) Products from the Reaction of a Racemic Mixture of L,L- and D,D-Py(AN_2H_3)$_2$ (0.055 mmol Each) with 1,4-Ph(NCS)$_2$ (0.1 mmol) in 1:1 (v/v) DMF/ACN at Different Temperatures and Reaction Time

			Yield of L,L,D,D-**1**		Total yield of L,L,L,L- and D,D,D,D-**1**	
Entry[a]	T/°C	Time/h	In solution[a]	Precipitates[b]	In solution[a]	Precipitates[b]
1[c]	25	24	-	-	-	-
2	50	24	14%	8%	14%	8%
3	80	24	8%	24%	8%	24%
4	90	24	20%	19%	16%	21%
5	100	24	16%	27%	10%	13%
6	110	24	13%	52%	1%	0%
7	120	24	-	-	-	-
8[c,d]	110	12	4%	66%	3%	7%
9[d]	110	16	2%	79%	0%	0%
10[d]	110	24	0%	71%	0%	0%

[a]The reaction mixture was filtered, and the filtrate was evaporated and dissolved in DMSO-d_6 for ^{1}H NMR analysis of the product ratio in solution. [b]The yields of the products as precipitates were determined by weighing the precipitates, dissolving in DMSO-d_6 and ^{1}H NMR analysis of the product ratio in the precipitates. [c]No precipitation observed. [d]Reactions 8−10 were conducted in pressure flasks.

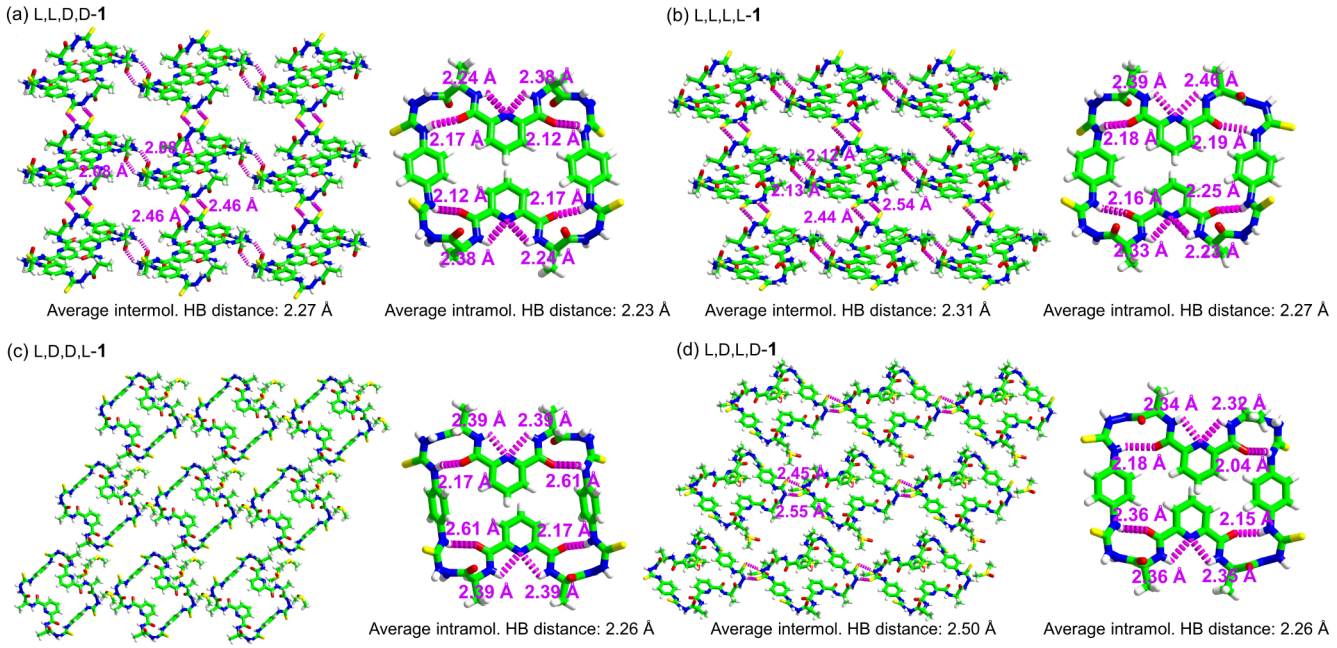

Figure 3. Comparison of intermolecular and intramolecular hydrogen bonds in the crystal structures of L,L,D,D-**1** (a), L,L,L,L-**1** (b), L,D,D,L-**1** (c), and L,D,L,D-**1** (d).

SEM (see Figure S2 for L,L,D,D-**1** and Figures S3−S5 for other stereoisomers), an indication of the strong and ordered intermolecular interactions. The yield of ca. 80% also implies that the reaction leading to heterochiral products is faster; otherwise, a yield of not higher than 50% would have been expected.

Similar heterochiral preference in the macrocycle synthesis was observed with the dihydrazide reactants containing phenylalanine (F) residues (Figure 1a). The reaction of racemic L,L- and D,D-Py(FN_2H_3)$_2$ with 1,4-Ph(NCS)$_2$ led exclusively to L,L,D,D-**2** in 78% yield under optimal conditions (Figure S6). Interestingly, mixed heterochiral macrocycles, L,L,D,D-AAFF (**3**) and D,D,L,L-AAFF (**4**), were obtained in yields of over 60% (Figures 1a). They are otherwise not easily accessible pseudoracemic macrocycles containing two L- and two D-amino acid residues of differing identities.

This heterochirality however is not that results from the heterochiral coupling observed in the acyclic bilateral systems containing the same heterochiral structural motif of 1,4-phenyldithioureas.[8] Macrocyclization reaction using the meso dihydrazide reactant (L,D-AA, Figure 1c) would in principle lead to L,D,D,L-**1** and L,D,L,D-**1** each in 50% possibility. However, we found that L,D,D,L-**1** was the only product in 53% isolated yield at a higher reaction temperature of 110 °C, despite a 73:27 molar ratio of L,D,D,L-**1** to L,D,L,D-**1** at a lower reaction temperature of 80 °C. In L,D,D,L-**1**, the two 1,4-benzenediamidothiourea motifs are both homochiral, either LL or DD, which is opposite to the acyclic systems where only the LD-heterochirality was observed due to the formation of *M*- and *P*-handed helices upon intermolecular stacking.[8] Therefore, it appears that the constraint of the macrocyclic molecules makes the intermacrocycle interactions not the same as those between acyclic molecules. It is also

https://doi.org/10.1021/jacsau.5c01669
JACS Au 2026, 6, 1319−1326

noteworthy that the heterochiral macrocycles L,L,D,D-**1** and L,D,D,L-**1** share the same arrangement profiles of the configurations along the 4-edge cyclic backbone, i.e., in parallel LL/DD and LD/LD edges containing, respectively, LL/DD and LD/LD amino acid residues (see structures of L,L,D,D-**1** and L,D,D,L-**1** in Figure 1a,c). This is different from the heterochiral giant cubic [8 + 12] cage,[3c] which precipitated from a reaction solution of poor solvent THF, with all edges being heterochiral. Of interest is that in good solvents, such as CH_2Cl_2, the obtained soluble products are homochiral [8 + 12] cages, and this behavior was well explained by an information entropy theory,[4c] which predicts heterochirality at lower temperatures. This is, again, opposite to what was observed here, where heterochirality is preferred at higher temperatures.

Precipitation of the reaction product from a high-temperature reaction solution implies that the solute−solute intermolecular interactions are strong. The crystalline structure of the precipitates (Figures S2−S5) suggests that the solute−solute interactions are strong and ordered, which is also supported by their easy crystallization. We performed thermogravimetric analyses (TGA) of the macrocycles and found that the decomposition temperatures of L,L,L,L/D,D,D,D-**1** (249 °C) and L,D,L,D-**1** (229 °C) are lower than those of the preferred L,L,D,D-**1** (278 °C) and L,D,D,L-**1** (271 °C) (Figures S7−S11, Table S1), confirming the higher thermostability of the preferentially formed macrocycles in the solid state.

Previously, we observed that homochiral L,L,L,L-**1** and D,D,D,D-**1** precipitated from the reaction solution at 90 °C during their respective syntheses (Figure S3). The present heterochiral product L,L,D,D-**1** precipitates from the reaction solution too, at a higher temperature of 110 °C. This implies stronger intermolecular interactions between the molecules of heterochiral product L,L,D,D-**1**. Single crystals of L,L,D,D-**1** were facilely obtained that allows for the X-ray diffraction crystal structure characterization (Figures 3a and S12). L,L,D,D-**1** crystallizes in *P*-1 space group (Table S2), with each L,L,D,D-**1** molecule showing a centrosymmetric conformation, contrasting the lack of such symmetry in the previously reported crystal structures of L,L,L,L-**1** and D,D,D,D-**1**, which actually take a distorted structure, three of the four methyl substituents of the alanine residues above the macrocycle plane while the fourth below (Figure 3 and Table S3 for β-turn parameters which differ quite much from each other). As with L,L,L,L-**1** and D,D,D,D-**1**, each molecule of L,L,D,D-**1** contains four β-turn structures maintained by 10-membered intramolecular hydrogen bonds, with its four methyl substituents being two above and two below the cyclic plane (Figure 3a). In the crystals, L,L,D,D-**1** molecules stack via strong intermolecular hydrogen bonds, including bifurcated pyridinedicarboxamide N−H···O═C hydrogen bonds along *a* axis, self-complementary thioureido N−H···S═C hydrogen bonds along *b* axis and self-complementary thioureido N−H···O═C (alanine) hydrogen bonds along *c* axis (Figures 3a, S13−S14). The intramolecular and intermolecular hydrogen bonding patterns in the crystals of L,L,D,D-**1** (Figures S15−S17) are similar to those in the homochiral counterparts L,L,L,L-**1**/D,D,D,D-**1**. However, we found that the hydrogen bonds in L,L,D,D-**1** are collectively stronger than those in L,L,L,L-**1** and D,D,D,D-**1** (Figure 3a,b, and Tables S3−S4), while the $\pi\cdots\pi$ stacking distances in the three structures are similar (Figure S17 and Table S5). The average intramolecular N−H···O═C distances and angles for L,L,D,D-**1** in the β-turns were 2.23 Å and 153°, respectively, whereas those for L,L,L,L-**1** were 2.27 Å and 153° and those for D,D,D,D-**1**, 2.26 Å and 153°. L,L,D,D-**1** also shows shorter intermolecular hydrogen bonds, with D-H···A distances determined to be 2.27 Å, compared with 2.31 for L,L,L,L-**1** and 2.29 for D,D,D,D-**1**. Similar crystal packing pattern stabilized by strong intermolecular hydrogen bonds was observed for L,L,D,D-**3** (Figures S18−S20). The crystal structure of L,D,D,L-**1** (Figures 3c, S21−S23) shows a centrosymmetric conformation with a symmetric distribution of four methyl substituents and four β-turns as with L,L,D,D-**1**, in which the intramolecular N−H···O═C distances and angles are 2.61 Å (β1 and β3) and 2.17 Å (β2 and β4) and 154° and 160°, respectively. The outward pointing NH donor and C═O/C═S acceptor groups of L,D,D,L-**1** form hydrogen bonds with the oxygen acceptor and the CH_3 donor groups of the DMSO solvents, respectively. Contrasting L,D,D,L-**1**, crystal structure of L,D,L,D-**1** shows a lack of symmetry in the macrocycle conformation, with its four β-turns being different in terms of their N−H···O═C distances (2.18, 2.04, 2.15, and 2.36 Å) and angles (149, 158, 155, and 153°) (Figures 3d, S24−S26). A set of self-complementary thioureido N−H···S═C hydrogen bonds were observed in the crystal packing, with the remaining outward pointing polar groups of L,D,L,D-**1** hydrogen bonded to solvent molecules (DMSO and ethyl acetate, with some highly disordered solvent-molecules treated with the PLATON SQUEEZE method). Overall, these results demonstrate an interesting trend that L,L,D,D- and L,D,D,L-macrocycles, the preferentially formed products, have centrosymmetric conformations in the solid state. By contrast, the unfavored L,L,L,L-, D,D,D,D- and L,D,L,D-macrocyclic products lack such symmetry in their solid states. Because crystals have periodic symmetry, molecules with high symmetry are often found to facilitate efficient molecular packing.[10] For example, the benefit of centrosymmetric molecular geometry in crystal packing was demonstrated by a study revealing that a small library of flexible molecules tends to crystallize in centrosymmetric conformations, despite the fact that, in some cases, these conformations are of higher energy than the alternative noncentrosymmetric conformations.[11] We thus hypothesized that the centrosymmetric feature of the L,L,D,D- and L,D,D,L-macrocycles leads to more efficient packing and consequently higher thermodynamic stability in the solid states compared to L,L,L,L-, D,D,D,D- and L,D,L,D-isomers, as supported by the TGA studies (Table S1). In addition, crystals of symmetric molecules possess greater entropies than crystals of unsymmetric analogues.[12] Thus, the information theory predicts that high reaction temperatures should favor the formation of symmetric L,L,D,D- and L,D,D,L-macrocycles as high-entropy crystalline products, consistent with our observation of temperature dependence (e.g., Table 1).

On the other hand, in solution where the macrocycle product exists discretely, the stability of the intramolecular hydrogen bonds was examined by varying solvent composition ^{1}H NMR studies. We used DMSO as a hydrogen bond-destabilizing solvent and monitor the changes of -NH signals upon increasing the fraction of DMSO in CH_3CN/DMSO binary mixtures. In our previous study of L,L,L,L-**1**, we have confirmed -NH^d and -NH^a as being involved in intramolecular hydrogen bonds in solution because their signals are less sensitive to increasing DMSO ratio compared with those of -NH^b and -NH^c (see Figure 1 for proton labeling).[7] Here, we

https://doi.org/10.1021/jacsau.5c01669
JACS Au 2026, 6, 1319−1326

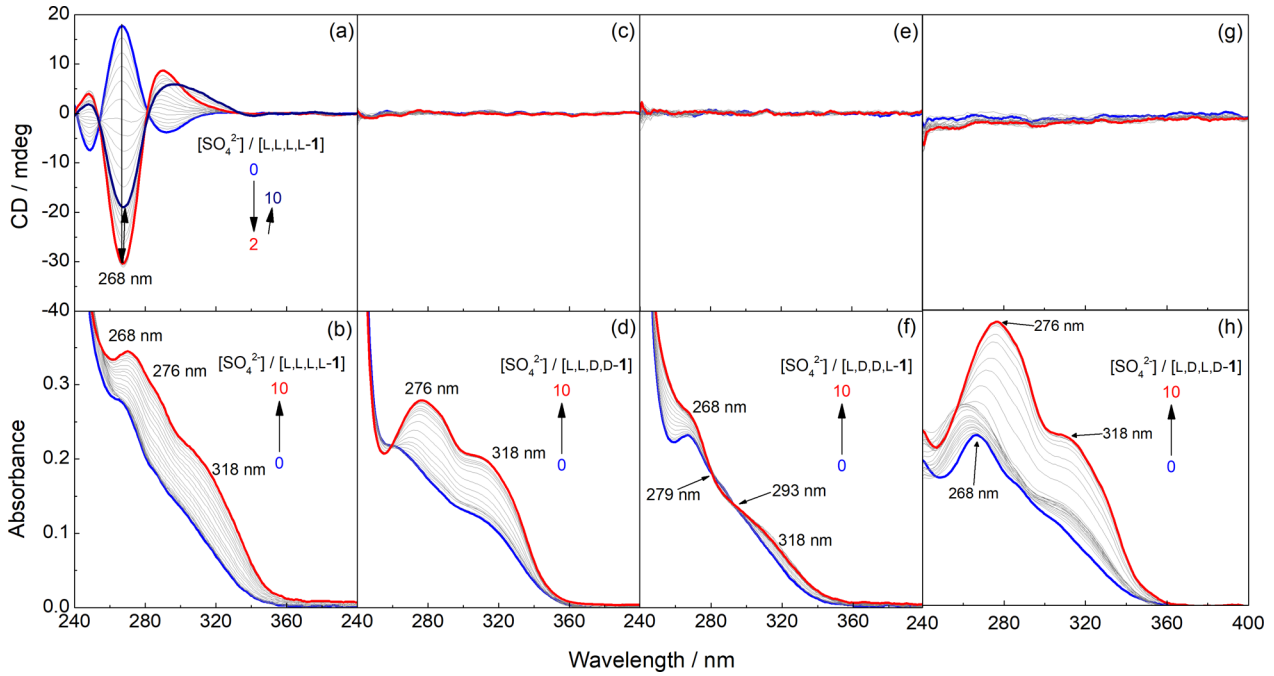

Figure 4. CD and absorption spectra of L,L,L,L-**1** (a,b), L,L,D,D-**1** (c,d), L,D,D,L-**1** (e,f), and L,D,L,D-**1** (h,g) in the presence of SO_4^{2-} of increasing concentration in 99.5:0.5 (v/v) CH_3CN/DMSO. L,L,D,D-, L,D,D,L-, and L,D,L,D-**1** are achiral, but both bear chiral centers. The absorption and CD spectra of L,L,L,L-**1** in the presence of SO_4^{2-} were taken from reference 7. [**1**] = 5 μM; $(n\text{-Bu})_4N^+$ salt of SO_4^{2-} was used.

performed these analyses to compare the intramolecular hydrogen bonds among the different macrocycles in solution. The -NH^d and -NH^a protons in L,L,L,L-**1** of increasing volume fractions of DMSO (10 to 100%) undergo changes in their chemical shifts by average slopes of −0.8 and 3.8 ppb/% DMSO, respectively.[7] These changes are slightly less pronounced than those observed in L,L,D,D-**1** under the same conditions, at −0.9 and 4.0 ppb/% DMSO, respectively, for -NH^d and -NH^a protons (Figures S27 and S28). These data indicate that the intramolecular hydrogen bonds within the homochiral L,L,L,L-**1** molecules are stronger than those in the heterochiral L,L,D,D-**1**, suggesting that the individual homochiral macrocycle in solution is more stable than the heterochiral counterpart, opposite of that observed in their crystals. Similarly, the intramolecularly hydrogen-bonded protons in L,D,L,D-**1** are less sensitive to changes in solvent composition (average slopes of −0.3 and 3.4 ppb/% DMSO for -NH^d and -NH^a, respectively, Figures S29 and S30) than those in L,D,D,L-**1** (average slopes of −0.8 and 3.6 ppb/% DMSO for -NH^d and -NH^a, respectively, Figures S31 and S32), again demonstrating stronger solution-state *intra*molecular hydrogen bonds of L,D,L,D-**1** than those of L,D,D,L-**1**, despite the latter being the preferentially formed macrocycle in the solid state. These results therefore suggest that the stronger *inter*molecular interactions between the centrosymmetric macrocycle product molecules than those of the non-centrosymmetric counterparts, rather than the stability of the individual macrocycles, dictate the cyclization outcome at higher temperatures. This is opposite to the case in which the reaction product exists as discrete species, in which a lower temperature favors the heterochiral macrocycle product.[2e]

The success of obtaining those heterochiral macrocycles provides a small library of the stereoisomers containing L,L,L,L-**1**, D,D,D,D-**1**, L,L,D,D-**1**, L,D,D,L-**1**, and L,D,L,D-**1**, allowing for the study of potential allosteric binding[13] to achiral species, sulfate anion here. Allosteric regulation was previously found in sulfate binding to L,L,L,L-**1** because the thiourea binding sites existed in a *cis,trans*-conformation[14] in the networked cyclic backbone and inverted to a *trans,trans*-conformation upon binding to SO_4^{2-} anion.[7] Figure 4 shows the absorption and CD spectra of L,L,L,L-**1**, L,L,D,D-**1**, L,D,D,L-**1**, and L,D,L,D-**1** in 99.5:0.5 (v/v) CH_3CN/DMSO in the presence of SO_4^{2-}. The absorption traces of them upon binding to SO_4^{2-} differ dramatically, demonstrating that the conformations of the anion-bound macrocycles are highly sensitive to the chiral centers. This is despite the fact that NMR titrations show all these new macrocyclic isomers bind SO_4^{2-} very strongly in that the original NMR signals weaken while new sets of signals develop (Figures S33−S35), similar to L,L,L,L-**1** that SO_4^{2-} binding results in a conformation inversion.[7] This agrees with the fact that the anion-binding sites in the macrocyclic backbone are networked (Figure 3) that the binding of an achiral anion to the chiral macrocycles or achiral macrocycles but bearing chiral centers is allosteric.[13] The ability of these macrocycles to bind anions with strong affinities, forming complexes with rich chirality-dependent optical properties points toward potential applications in chirality separation and information storage.

CONCLUSIONS

We developed a highly effective self-sorting system in which strong intermolecular interactions between the reaction product molecules direct the reaction pathway to exclusively form L,L,D,D- or L,D,D,L-peptidomimetic macrocycles, when racemic or meso dihydrazide reactants were used. This was observed at high temperatures and in competitive solvents, despite the hydrogen-bonding nature of the intermacrocycle stacking. The chiral preference in the reaction products, i.e., L,L,D,D-**1** against L,L,L,L-/D,D,D,D-**1** and L,D,D,L-**1** against L,D,L,D-**1**, happens despite the fact that the preferred

https://doi.org/10.1021/jacsau.5c01669
JACS Au 2026, 6, 1319−1326

macrocycles that exist in individual species in the solution phase are slightly less stable. The preferred macrocycles of L,L,D,D- or L,D,D,L-configuration (clockwise) share a centrosymmetric feature and the same pattern of the four edges, parallel LL/DD and LD/LD, that favor the stronger intermolecular interactions. This chiral preference is observed in the *covalent* macrocyclization reactions, where the product molecule exists in the *aggregate* state of strong *inter*molecular interactions. This phenomenon is distinct with regard to most of the hitherto reported reactions that are controlled by the *intra*molecular interaction profiles in the transition state and the product molecule. Our preliminary screening of the scope of the present scheme shows that the synthetic protocol is applicable to heterochiral macrocycles with varying amino acid residues and/or aromatic arms, allowing the access to a variety of macrocyclic stereoisomers. We believe that our results reported here would inspire explorations of the reactions of chiral species leading to products and/or involving the transition states which are, more generally, in aggregated forms.[15]

■ ASSOCIATED CONTENT

Supporting Information

The Supporting Information is available free of charge at https://pubs.acs.org/doi/10.1021/jacsau.5c01669.

Detailed synthetic procedures (Schemes S1−S9), characterization (Figures S36−S76), SEM micrographs, NMR analyses, thermogravimetric analyses, X-ray crystallography, and UV−vis absorption spectra (PDF)

Accession Codes

Deposition Numbers 2372932, 2372936, 2372938, and 2491944 contain the supplementary crystallographic data for this paper. These data can be obtained free of charge via the joint Cambridge Crystallographic Data Centre (CCDC) and Fachinformationszentrum Karlsruhe Access Structures service.

■ AUTHOR INFORMATION

Corresponding Authors

Liuyin Jiang − *Department of Chemical and Biological Engineering, College of Chemistry and Chemical Engineering, Institute of Flexible Elec-tronics, and The MOE Key Laboratory of Spectrochemical Analysis and Instrumentation, Xiamen University, Xiamen 361005, China*; Email: lyjiang@xmu.edu.cn

Xin Wu − *School of Pharmaceutical Sciences and the MOE Key Laboratory of Spectrochemical Analysis and Instrumentation, Xiamen University, Xiamen 361102, China*; orcid.org/0000-0002-7715-8784; Email: xin.wu@xmu.edu.cn

Tao Jiang − *Department of Chemistry, College of Chemistry and Chemical Engineering and the MOE Key Laboratory of Spectrochemical Analysis and Instrumentation, Xiamen University, Xiamen 361005, China*; orcid.org/0000-0003-3042-1247; Email: tjiang6@xmu.edu.cn

Yun-Bao Jiang − *Department of Chemistry, College of Chemistry and Chemical Engineering and the MOE Key Laboratory of Spectrochemical Analysis and Instrumentation, Xiamen University, Xiamen 361005, China*; orcid.org/0000-0001-6912-8721; Email: ybjiang@xmu.edu.cn

Authors

Zhen-Sheng Huang − *Department of Chemistry, College of Chemistry and Chemical Engineering and the MOE Key Laboratory of Spectrochemical Analysis and Instrumentation, Xiamen University, Xiamen 361005, China*

Wen-Rong Wang − *Department of Chemistry, College of Chemistry and Chemical Engineering and the MOE Key Laboratory of Spectrochemical Analysis and Instrumentation, Xiamen University, Xiamen 361005, China*

Fang-Hong Yang − *Department of Chemistry, College of Chemistry and Chemical Engineering and the MOE Key Laboratory of Spectrochemical Analysis and Instrumentation, Xiamen University, Xiamen 361005, China*

Fei Gou − *Department of Chemistry, College of Chemistry and Chemical Engineering and the MOE Key Laboratory of Spectrochemical Analysis and Instrumentation, Xiamen University, Xiamen 361005, China*

Chi-Cheng Qiu − *Department of Chemistry, College of Chemistry and Chemical Engineering and the MOE Key Laboratory of Spectrochemical Analysis and Instrumentation, Xiamen University, Xiamen 361005, China*

Yang-Yu Tai − *Department of Chemistry, College of Chemistry and Chemical Engineering and the MOE Key Laboratory of Spectrochemical Analysis and Instrumentation, Xiamen University, Xiamen 361005, China*

Xiao-Sheng Yan − *School of Pharmaceutical Sciences and the MOE Key Laboratory of Spectrochemical Analysis and Instrumentation, Xiamen University, Xiamen 361102, China*; orcid.org/0000-0002-4207-9752

Complete contact information is available at: https://pubs.acs.org/10.1021/jacsau.5c01669

Author Contributions

[#]Z.-S.H. and W.-R.W. contributed equally.

Funding

We greatly appreciate the financial support from the NSF of China (22241503, 22371240, and 92356308), the MOE of China Fundamental Research Funds for the Central Universities (20720220005 and 20720220121), and Xiamen Municipal Bureau of Science and Technology (3502Z20251005).

Notes

The authors declare no competing financial interest.

■ REFERENCES

(1) (a) Deng, M.; Yu, J.; Blackmond, D. G. Kinetic Resolution as a General Approach to Enantioenrichment in Prebiotic Chemistry. *Acc. Chem. Res.* **2024**, *57*, 2234−2244. (b) Deng, M.; Yu, J.; Blackmond, D. G. Symmetry breaking and chiral amplification in prebiotic ligation reactions. *Nature* **2024**, *626*, 1019−1024.

(2) (a) Lin, M.; Bian, L.; Chen, Q.; Xu, H.; Liu, Z.; Zhu, K. Cyclization of an Achiral Flipping Panel to Homochiral Tubes Exhibiting Circularly Polarized Luminescence. *Angew. Chem., Int. Ed.* **2023**, *62* (28), No. e202303035. (b) Zhang, G.-W.; Li, P.-F.; Meng, Z.; Wang, H.-X.; Han, Y.; Chen, C.-F. Triptycene-Based Chiral Macrocyclic Hosts for Highly Enantioselective Recognition of Chiral Guests Containing a Trimethylamino Group. *Angew. Chem., Int. Ed.* **2016**, *55*, 5304−5308. (c) Liu, G.; Guo, S.; Liu, L.; Fan, Y.; Lian, Z.; Chen, X.; Jiang, H. Shape-Persistent Triptycene-Derived Pillar[6]-arenes: Synthesis, Host−Guest Complexation, and Enantioselective Recognitions of Chiral Ammonium Salts. *J. Org. Chem.* **2023**, *88*, 10171−10179. (d) Han, X.-N.; Li, P.-F.; Han, Y.; Chen, C.-F. Enantiomeric Water-Soluble Octopus[3]arenes for Highly Enantio-

selective Recognition of Chiral Ammonium Salts in Water. *Angew. Chem Int Ed.* **2022**, *61* (21), No. e202202527. (e) Sisco, S. W.; Moore, J. S. Homochiral Self-Sorting of BINOL Macrocycles. *Chem. Sci.* **2014**, *5* (1), 81−85.
(3) (a) Chen, Q.; Li, Z.; Lei, Y.; Chen, Y.; Tang, H.; Wu, G.; Sun, B.; Wei, Y.; Jiao, T.; Zhang, S.; et al. The sharp structural switch of covalent cages mediated by subtle variation of directing groups. *Nat. Commun.* **2023**, *14* (1), 4627. (b) Wang, Z.; Zhang, Q.-P.; Guo, F.; Ma, H.; Liang, Z.-H.; Yi, C.-H.; Zhang, C.; Chen, C.-F. Self-similar chiral organic molecular cages. *Nat. Commun.* **2024**, *15* (1), 670. (c) Wang, X.; Wang, Y.; Yang, H.; Fang, H.; Chen, R.; Sun, Y.; Zheng, N.; Tan, K.; Lu, X.; Tian, Z.; et al. Assembled molecular face-rotating polyhedra to transfer chirality from two to three dimensions. *Nat. Commun.* **2016**, *7* (1), 12469.
(4) (a) Wu, K.; Benchimol, E.; Baksi, A.; Clever, G. H. Non-statistical assembly of multicomponent [Pd_2ABCD] cages. *Nat. Chem.* **2024**, *16*, 584−591. (b) Wagner, P.; Rominger, F.; Gross, J. H.; Mastalerz, M. Solvent-Controlled Quadruple Catenation of Giant Chiral [8 + 12] Salicylimine Cubes Driven by Weak Hydrogen Bonding. *Angew. Chem., Int. Ed.* **2023**, *62* (14), No. e202217251. (c) Wagner, P.; Rominger, F.; Zhang, W. S.; Gross, J. H.; Elbert, S. M.; Schröder, R. R.; Mastalerz, M. Chiral Self-sorting of Giant Cubic [8 + 12] Salicylimine Cage Compounds. *Angew. Chem., Int. Ed.* **2021**, *60*, 8896−8904. (d) Beaudoin, D.; Rominger, F.; Mastalerz, M. Chiral Self-sorting of [2 + 3] Salicylimine Cage Compounds. *Angew. Chem., Int. Ed.* **2017**, *56*, 1244−1248.
(5) Ponnuswamy, N.; Cougnon, F. B. L.; Clough, J. M.; Pantoş, G. D.; Sanders, J. K. M. Discovery of an Organic Trefoil Knot. *Science* **2012**, *338*, 783−785.
(6) Golec, J. C.; Tan, D.-H.; Yamazaki, K.; Tiekink, E. H.; Christensen, K. E.; Hamlin, T. A.; Dixon, D. J. Catalytic enantioselective synthesis of alkylidenecyclopropanes. *Nature* **2025**, *645*, 932−938. (b) Gair, J. J.; Isomura, M.; Wagen, C. C.; Strassfeld, D. A.; Jacobsen, E. N. Enantioselective Ring Opening of Azetidines via Charge Recognition in Hydrogen-Bond-Donor Catalysis. *J. Am. Chem. Soc.* **2025**, *147*, 6378−6383. (c) Lovinger, G. J.; Sak, M. H.; Jacobsen, E. N. Catalysis of an S_N Pathway by Geometric Preorganization. *Nature* **2024**, *632*, 1052−1059. (d) Wang, M.; Liu, S.; Liu, H.; Wang, Y.; Lan, Y.; Liu, Q. Asymmetric Hydrogenation of Ketimines with Minimally Different Alkyl Groups. *Nature* **2024**, *631*, 556−562. (e) Dang, Q.-D.; Deng, Y.-H.; Sun, T.-Y.; Zhang, Y.; Li, J.; Zhang, X.; Wu, Y.-D.; Niu, D. Catalytic Glycosylation for Minimally Protected Donors and Acceptors. *Nature* **2024**, *632*, 313−319.
(7) Gou, F.; Shi, D.; Kou, B.-H.; Li, Z.; Yan, X.-S.; Wu, X.; Jiang, Y.-B. One-pot cyclization to large peptidomimetic macrocycles by in situ generated β-turn enforced folding. *J. Am. Chem. Soc.* **2023**, *145*, 9530−9539.
(8) Yan, X.; Cao, J.; Luo, H.; Li, Z.; Cao, Z.; Mo, Y.; Jiang, Y.-B. Heterochiral coupling to bilateral β-turn structured azapeptides bearing two remote chiral centers. *Nat. Commun.* **2024**, *15* (1), 9271.
(9) (a) Liu, X.; Weinert, Z. J.; Sharafi, M.; Liao, C.; Li, J.; Schneebeli, S. T. Regulating Molecular Recognition with C-Shaped Strips Attained by Chirality-Assisted Synthesis. *Angew. Chem., Int. Ed. Engl.* **2015**, *54*, 12772−12776. (b) Beaudoin, D.; Rominger, F.; Mastalerz, M. Chirality-Assisted Synthesis of a Very Large Octameric Hydrogen-Bonded Capsule. *Angew. Chem., Int. Ed.* **2016**, *55*, 15599−15603. (c) Singh, Y.; Schuldt, M. P.; Rominger, F.; Mastalerz, M. High-Yielding Nanobelt Formation by Chirality-Assisted Synthesis. *Angew. Chem., Int. Ed.* **2024**, *64*, No. e202414059.
(10) Pidcock, E.; Motherwell, W. D. S.; Cole, J. C. A database survey of molecular and crystallographic symmetry. *Acta Crystallogr. B* **2003**, *59*, 634−640.
(11) Thompson, H. P. G.; Day, G. M. Which conformations make stable crystal structures? Mapping crystalline molecular geometries to the conformational energy landscape. *Chem. Sci.* **2014**, *5*, 3173−3182.
(12) Pinal, R. Effect of molecular symmetry on melting temperature and solubility. *Org. Biomol. Chem.* **2004**, *2*, 2692−2699.
(13) (a) Takeuchi, M.; Ikeda, M.; Sugasaki, A.; Shinkai, S. Molecular Design of Artificial Molecular and Ion Recognition Systems with Allosteric Guest Responses. *Acc. Chem. Res.* **2001**, *34*, 865−873. (b) Shinkai, S.; Ikeda, M.; Sugasaki, A.; Takeuchi, M. Positive Allosteric Systems Designed on Dynamic Supramolecular Scaffolds: Toward Switching and Amplification of Guest Affinity and Selectivity. *Acc. Chem. Res.* **2001**, *34*, 494−503. (c) Hunter, C.; Anderson, H. L. What is cooperativity? *Angew. Chem., Int. Ed.* **2009**, *48*, 7488−7499.
(14) (a) Li, A.-F.; Wang, J.-H.; Wang, F.; Jiang, Y.-B. Anion complexation and sensing using modified urea and thiourea based receptors. *Chem. Soc. Rev.* **2010**, *39*, 3729−3745. (b) Wang, Q.; Liu, S.-Y.; Jiang, Y.-B. *N*-Acylamino acid amidothiourea: A versatile chiral helical building block. *Acc. Chem. Res.* **2025**, *58*, 3046−3059.
(15) (a) Zheng, T.; Nöthling, N.; Wang, Z.; Mitschke, B.; Leutzsch, M.; List, B. A solid noncovalent organic double-helix framework catalyzes asymmetric [6 + 4] cycloaddition. *Science* **2024**, *385*, 765−770. (b) Hinge, S.; Kundu, S.; Niemeyer, J. The impact of supramolecular self-association of organocatalysts on catalytic performance. *Nat. Rev. Chem.* **2025**, *9*, 688−706.

https://doi.org/10.1021/jacsau.5c01669
JACS Au 2026, 6, 1319−1326